REVISION 1

Vladykinite, $Na_3Sr_4(Fe^{2+}Fe^{3+})Si_8O_{24}$: a new complex sheet silicate from peralkaline rocks of the Murun complex, eastern Siberia, Russia

ANTON R. CHAKHMOURADIAN[1]*, MARK A. COOPER[1], NEIL BALL[1], EKATERINA P. REGUIR[1], LUCA MEDICI[2], YASSIR ABDU[1] AND ANTON A. ANTONOV[3]

[1] Department of Geological Sciences, University of Manitoba, Winnipeg, MB, R3T 2N2, Canada
[2] Istituto di Metodologie per l'Analisi Ambientale, Tito Scalo, 85050 Potenza, Italy
[3] Centre for Isotopic Research, VSEGEI, 74 Sredniy Prospect, St. Petersburg, 199106, Russia
* Corresponding author; e-mail: chakhmou@cc.umanitoba.ca

ABSTRACT

Vladykinite, ideally $Na_3Sr_4(Fe^{2+}Fe^{3+})Si_8O_{24}$, is a new complex sheet silicate occurring as abundant prismatic crystals in a dike of coarse-grained peralkaline feldspathoid syenite in the north-central part of the Murun complex in eastern Siberia, Russia (Lat. 58° 22′ 48″ N; Long. 119° 03′ 44″ E). The new mineral is an early magmatic phase associated with aegirine, potassium feldspar, eudialyte, lamprophyllite and nepheline; strontianite (as pseudomorphs after vladykinite) and K-rich vishnevite are found in the same assemblage, but represent products of late hydrothermal reworking. Vladykinite is brittle, has a Mohs hardness of 5 and distinct cleavage on {100}. In thin section, it is colorless, biaxial negative [α = 1.624(2), β = 1.652(2), γ = 1.657(2), $2V_{meas}$ = 44(1)°, $2V_{calc}$ = 45(1)°] and shows an optic orientation consistent with its structural characteristics ($X \wedge a = 5.1°$ in β obtuse, $Z \wedge c = 4.7°$ in β acute, $Y = b$). The Raman spectrum of vladykinite consists of the following vibration modes (listed in order of decreasing intensity): 401, 203, 465, 991, 968, 915, 348, 167, 129, 264, 1039 and 681 cm^{-1}; O-H signals were not detected. The Mössbauer spectrum indicates that both Fe^{2+} and Fe^{3+} are present in the

mineral ($Fe^{3+}/Fe_{\Sigma} = 0.47$), and that both cations occur in a tetrahedral coordination. The mean chemical composition of vladykinite (acquired by wavelength-dispersive X-ray spectrometry and laser-ablation inductively-coupled-plasma mass-spectrometry), with Fe_{Σ} recast into Fe^{2+} and Fe^{3+} in accord with the Mössbauer data, gives the following empirical formula calculated to 24 oxygen atoms:

$(Na_{2.45}Ca_{0.56})_{\Sigma 3.01}(Sr_{3.81}K_{0.04}Ba_{0.02}La_{0.02}Ce_{0.01})_{\Sigma 3.90}(Fe^{2+}_{0.75}Fe^{3+}_{0.66}Mn_{0.26}Zn_{0.16}Al_{0.12}Mg_{0.05}Ti_{0.01})_{\Sigma 2.01}(Si_{7.81}Al_{0.19})_{\Sigma 8.00}O_{24}$. The mineral is monoclinic, space group $P2_1/c$, $a = 5.21381(13)$, $b = 7.9143(2)$, $c = 26.0888(7)$ Å, $\beta = 90.3556(7)°$, $V = 1076.50(5)$ Å^3, $Z = 2$. The ten strongest lines in the powder X-ray diffraction pattern are [d_{obs} in Å (I) (hkl)]:
2.957 (100) ($\bar{1}23$, 123); 2.826 (100) ($\bar{1}17$, 117); 3.612 (58) ($\bar{1}14$, 114); 3.146 (37) (120); 2.470 (32) (210, 01.10); 4.290 (30) ($\bar{1}11$, 111); 3.339 (30) ($\bar{1}06$, 115, 106); 2.604 (28) (200); 2.437 (25) (034); 1.785 (25) (21.10, $\bar{2}34$). The structure of vladykinite, refined by single-crystal techniques on the basis of 3032 reflections with $F_o > 4\sigma F_o$ to $R_1 = 1.6\%$, consists of tetrahedral sheets parallel to (100) and consisting of $(Si_8O_{24})^{16-}$ units incorporating four-membered silicate rings and joined into five- and eight-membered rings by sharing vertices with larger tetrahedra hosting Fe^{2+}, Fe^{3+}, Mn, Zn, Al, Mg and Ti. Larger cations (predominantly Na, Sr and Ca) are accommodated in octahedral and square-antiprismatic interlayer sites sandwiched between the tetrahedral sheets. Structural relations between vladykinite and other sheet silicates incorporating four-, five- and eight-membered rings are discussed. The name vladykinite is in honor of Nikolay V. Vladykin (Vinogradov Institute of Geochemistry, Russia), in recognition of his contribution to the study of alkaline rocks. Holotype and cotype specimens of the mineral were deposited in the Robert B. Ferguson Museum of Mineralogy in Winnipeg, Canada.

Keywords: Vladykinite, new mineral, sheet silicate, peralkaline rocks, Murun complex, Yakutia, Russia

INTRODUCTION

Potassic peralkaline syenites (wt.% K_2O > wt.% Na_2O; mol.% Na_2O+K_2O > mol.% Al_2O_3) are an uncommon type of igneous rocks that, in extreme cases, contain an appreciable proportion of kalsilite ($KAlSiO_4$) or leucite (typically replaced by kalsilite-orthoclase intergrowths). Notable examples of these rocks occur in the Murun, Synnyr, Yaksha and Yuzhnosakunsky alkaline complexes in eastern Siberia, and at Khibiny in Kola Peninsula, Russia (Kostyuk et al. 1990; Ageeva and Borutzky 2004; Pakhomovsky et al. 2009). These syenites, their associated metasomatites and pegmatites host a plethora of exotic accessory minerals enriched in K, Sr or Ba, which are exceedingly rare or unknown in other rock types. For example, out of some 160 minerals reported from the Murun complex, fifty-seven contain essential K, Ba or Sr, including several species so far endemic to this locality (for details and bibliography, see Appendix 1, online). It is important to note here that most of these exotic minerals are not at all rare at Murun and locally gain the status of rock-forming constituents; a good understanding of their crystal chemistry and paragenetic relations is thus essential to the understanding of the petrogenesis of their host rocks.

In her study of peralkaline syenitic dikes from the Murun complex, Reguir (2001) briefly described a previously unknown Na-Fe-Sr silicate (pp. 162-163), but the dearth of available material precluded its detailed examination. Complete characterization of this mineral became possible only when additional samples were provided to us by Professor Nikolay V. Vladykin (Vinogradov Institute of Geochemistry in Irkutsk, Russia), who had also recognized this silicate as a potential new species. The new mineral and its name have been approved by the Commission on New Minerals, Nomenclature and Classification of the International Mineralogical Association (IMA 2011-052). The name vladykinite (владыкинит) was chosen in honor of Nikolay V. Vladykin (b. 1944), in recognition of his contribution to the geochemistry, petrology and mineralogy of alkaline rocks, including the Murun complex (Vladykin 1981, 1997, 2009; Mitchell and Vladykin 1993, 1996; Vladykin and Tsaruk 2003). Holotype and cotype specimens (unmounted and epoxy-mounted grains, polished thin sections and the crystal used for

structure refinement) were deposited in the Robert B. Ferguson Museum of Mineralogy at the University of Manitoba (Winnipeg, Canada) under catalogue number M7853.

GEOLOGICAL PROVENANCE AND PARAGENESIS

The Murun alkaline complex is a large (~60 km^2) composite pluton of Cretaceous age emplaced in Archean high-grade metamorphic rocks and Neoproterozoic clastic and carbonate sedimentary rocks (Kostyuk et al. 1990; Konev et al. 1996). The complex comprises a wide variety of igneous, metasomatic and hydrothermal rocks, but the most volumetrically significant are alkali-rich ultramafites, feldspathoid and quartz syenites, and their extrusive analogues (phonolites, trachytes, leucitites). Murun is known widely as the type locality of the purple gemstone charoite (Evdokimov 1995) and several other compositionally and structurally unusual minerals (Appendix 1, online).

Vladykinite was identified in a dike of coarse-grained mesocratic feldspathoid syenite (lujavrite) at Mt. Maly Murun in the north-central part of the complex. Geographically, Maly Murun is situated in southwestern Yakutia near its administrative border with the Irkutsk Region (Lat. 58° 22′ 48″ N; Long. 119° 03′ 44″ E). The host dike, measuring ~2-3 m in width and 20 m in length, comprises aegirine, potassium feldspar, K-Sr-bearing eudialyte, vladykinite, lamprophyllite, nepheline, strontianite and K-rich vishnevite, listed approximately in order of decreasing modal abundance (for formulae, see Appendix 1, online). Note that the cancrinite-group phase tentatively identified here as vishnevite is stoichiometrically close to pitiglianoite, $Na_6K_2Si_6Al_6O_{24}(SO_4)\cdot 2H_2O$; the two minerals can be distinguished only on the basis of structural data (Pekov et al. 2011), which are currently unavailable. In the Maly Murun lujavrite, vladykinite is relatively abundant, locally composing up to 5% of its volume. The mineral occurs as pointed prismatic crystals of brown color with a rhombic to pseudohexagonal cross-section perpendicular to the length, as well as parallel and radiating clusters of such crystals (Fig. 1a). The size of individual grains does not exceed a few mm in length and 0.5 mm in width. In hand-specimen, vladykinite resembles acicular titanite common in feldspathoid syenites (but

uncommon in their peralkaline varieties); the two minerals, however, differ in their optical properties (see below). The majority of crystals are partially or completely pseudomorphed by strontianite (Fig. 1b).

PHYSICAL AND OPTICAL PROPERTIES

The new mineral is macroscopically pinkish to grayish brown, with a vitreous luster and a white streak. It is brittle, has a Mohs hardness of 5 and a distinct cleavage on {100}. The specific gravity of vladykinite could not be measured, but is greater than that of di-iodomethane (3.22). The density, calculated on the basis of the chemical and crystallographic data (see below), is 3.51 g/cm^3. In thin section, the mineral is colorless, non-pleochroic, and shows a moderate positive relief. The optical properties, determined with a spindle stage, are as follows: α = 1.624(2), β = 1.652(2), γ = 1.657(2), $2V_{meas}$ = 44(1)°, $2V_{calc}$ = 45(1)°. Vladykinite is biaxial negative and shows the following optic orientation: X^*a* = 5.1° (β obtuse), Z^*c* = 4.7° (β acute), Y = *b*. Based on these properties, vladykinite can be readily distinguished from titanite, which has a much higher relief and birefringence, larger extinction angle (Z^*c* ≈ 50°), is pleochroic and biaxial positive (Deer et al. 1997). The calculated Gladstone-Dale compatibility index is 0.023 (excellent).

The micro-Raman spectrum, measured on the grain subsequently used for single-crystal analysis (Fig. 2), is complex and consists of lattice vibrations in the 100-350 cm^{-1} range and a series of Si-O and Fe-O modes between 400 and 1100 cm^{-1}. Because O-H stretching vibrations (3300-3600 cm^{-1}) were not observed, the presence of structural water or hydroxyl groups in this mineral can be conclusively ruled out.

MÖSSBAUER SPECTROSCOPY

Because Fe was identified as one of the major components in energy-dispersive X-ray spectra of vladykinite, the structural state of Fe was investigated using Mössbauer spectroscopy. The measurements were done at room temperature with a ^{57}Co(Rh) point source, using an Fe foil

for the spectrometer calibration. The ^{57}Fe Mössbauer spectrum, collected from several grains extracted from the holotype sample, indicates the presence of two active species, Fe^{2+} (solid line subspectrum in Fig. 3) and Fe^{3+} (dashed line). Consequently, the spectrum was fitted using a Voigt-based quadrupole-splitting distribution method to a model based on two species, each represented by a single Gaussian component. The refined parameters for the center shift (CS) relative to α-Fe at room temperature, and the quadrupole splitting (QS) are as follows: CS = 1.01(1) mm/s, QS = 2.77(3) mm/s for Fe^{2+}; and CS = 0.23(7) mm/s, QS = 0.87(9) mm/s for Fe^{3+}. The CS values indicate that both Fe^{2+} and Fe^{3+} occur in a tetrahedral coordination. Assuming equal recoil-free fractions for both species, the calculated Fe^{3+}/Fe_{Σ} ratio is 0.47(5).

CHEMICAL COMPOSITION

The chemical composition of vladykinite was initially determined by wavelength-dispersive X-ray spectrometry (WDS) using a CAMECA SX 100 fully automated electron-microprobe operated at an accelerating voltage of 15 kV and a beam current of 10 nA. Several crystals were analyzed with a 10-μm beam and found to show little compositional variation (Table 1). The following standards were employed for the analysis: albite (Na), andalusite (Al), diopside (Ca, Si), fayalite (Fe), forsterite (Mg), gahnite (Zn), orthoclase (K), spessartine (Mn), titanite (Ti), synthetic $SrTiO_3$ (Sr), $LaPO_4$ (La) and $CePO_4$ (Ce). In addition, F, Cl, Cr, Y, Zr, Nb, Ba, Pr, Nd, Sm, Ta and Th were sought, but found not to be present at levels detectable by WDS.

Vladykinite was also analyzed by laser-ablation inductively-coupled-plasma mass-spectrometry (LA-ICP-MS) using a 213-nm Nd-YAG Merchantek laser connected to a Thermo Finnigan Element 2 sector-field mass-spectrometer. All measurements were performed using a beam size of 30 μm, laser-energy density of ca. 5.45 J/cm^2 and repetition rate of 10 Hz. Ablation was done in Ar and He atmospheres, and the rate of oxide production was monitored during instrument tuning by measuring the ThO/Th ratio and kept below 0.2%. Synthetic glass standard NIST SRM 610 was employed for calibration and quality control. After taking into account potential spectral overlaps and molecular interferences, the following isotopes were chosen for

163 analysis: ^{25}Mg, ^{29}Si, ^{45}Sc, ^{51}V, ^{55}Mn, ^{59}Co, ^{60}Ni, ^{66}Zn, ^{85}Rb, ^{89}Y, ^{90}Zr, ^{93}Nb, ^{137}Ba, ^{139}La, ^{140}Ce,
164 ^{141}Pr, ^{146}Nd, ^{147}Sm, ^{151}Eu, ^{155}Gd, ^{159}Tb, ^{163}Dy, ^{165}Ho, ^{166}Er, ^{169}Tm, ^{172}Yb, ^{175}Lu, ^{178}Hf, ^{181}Ta,
165 ^{208}Pb, ^{232}Th, ^{238}U. All analyses were performed in a low-resolution mode (~300) using Pt
166 skimmer and sample cones. Data reduction was carried out online using the GLITTER software
167 (van Achterbergh et al. 2001). The Si concentrations determined by WDS show the least
168 variation around the mean value (Table 1) and were chosen as an internal standard for all
169 analyses. The quality control was achieved by keeping the fractionation at less than 10% and
170 fractionation/error ratio at < 3. The following elements were not detectable by LA-ICP-MS (their
171 approximate lower detection limits in ppm are given in parentheses): Ni (2), Rb (0.6), Zr (0.5),
172 Nb (0.5), Tb (0.1), Dy (0.2), Ho (0.05), Er (0.2), Tm (0.05), Yb (0.2), Lu (0.05), Hf (0.1), Ta
173 (0.05). For those elements that were quantified by both WDS and LA-ICP-MS, their measured
174 values are within the estimated standard deviation of each other (see Mg, Mn, Zn, La and Ce in
175 Table 1).

176 The mean chemical analysis of vladykinite, based on WDS (Na, Al, Si, Ca, Ti, Fe and Sr)
177 and LA-ICP-MS (Mg, Mn, Zn, La, Ce, Pr, Nd, Ba) data, with Fe_{Σ} recast into Fe^{2+} and Fe^{3+} in
178 accord with the Mössbauer data (4.76 wt.% FeO and 4.69 wt.% Fe_2O_3), gives the following
179 empirical formula calculated to 24 oxygen atoms: $(Na_{2.451}Ca_{0.557})_{\Sigma 3.008}(Sr_{3.805}K_{0.038}Ba_{0.015}La_{0.023}$
180 $Ce_{0.014}Pr_{0.001}Nd_{0.001})_{\Sigma 3.897}(Fe^{2+}_{0.746}Fe^{3+}_{0.662}Mn_{0.260}Zn_{0.164}Al_{0.118}Mg_{0.047}Ti_{0.014})_{\Sigma 2.011}(Si_{7.813}$
181 $Al_{0.187})_{\Sigma 8.000}O_{24}$. From crystal-chemical considerations (see **CRYSTAL STRUCTURE**), two
182 alternative end-member formulae can be proposed for vladykinite: $Na_3Sr_4(Fe^{2+}Fe^{3+})Si_8O_{24}$ or
183 $(Na_2Ca)Sr_4Fe^{2+}_2Si_8O_{24}$. These two expressions differ in the content of the Na and Fe sites and are
184 related to each other via the coupled substitution $Na^+ + Fe^{3+} \Leftrightarrow Ca^{2+} + Fe^{2+}$. Because the
185 trivalent-cation content in the Fe site (0.78 atoms per formula unit, apfu) is significantly in
186 excess of the Ca content in the Na sites (0.56 apfu), we give preference to the idealized formula
187 $Na_3Sr_4(Fe^{2+}Fe^{3+})Si_8O_{24}$.
188
189

CRYSTAL STRUCTURE

Single-crystal data were acquired with a Bruker D8 three-circle diffractometer equipped with a rotating anode generator (Mo$K\alpha$ radiation), multi-layer optics incident beam path and an APEX-II charge-coupled-device (CCD) detector. A sphere of X-ray diffraction data was collected to $2\theta = 60^{o}$ at 5 s per 0.2^{o} frame and a crystal-to-detector distance of 5 cm. The unit-cell parameters were obtained by least-squares refinement of 9873 reflections with $I > 10\sigma I$. Of 25682 total reflections, there are 11807 individual reflections within the Ewald sphere, including 3159 unique data; the Laue-merging R value is 1.5% in 2/m. Systematically absent reflections are consistent with the space group $P2_1/c$. The structure of vladykinite was refined on the basis of 3032 reflections with $F_o > 4\sigma F_o$ to $R_1 = 1.6\%$ (for a fully anisotropic model). The refined unit-cell parameters are: $a = 5.21381(13)$, $b = 7.9143(2)$, $c = 26.0888(7)$ Å, $\beta = 90.3556(7)°$, $V = 1076.50(5)$ Å^3, $Z = 2$. Although the departure in β from 90^{o} is small, the Laue-merging R value of 24% for *mmm* shows that the X-ray intensity data are inconsistent with orthorhombic symmetry (see **DISCUSSION**).

The crystal structure of vladykinite consists of complex tetrahedral sheets parallel to (100) and consisting of $(Si_8O_{24})^{16-}$ units incorporating four-membered silicate rings joined into five- and eight-membered rings by sharing vertices with larger tetrahedra hosting Fe, Mn, Zn, Al and Mg. The overall topology of the sheet can be formulated as $4^1 5^4 8^1$. Larger cations (predominantly Na, Sr and Ca) are accommodated in a variety of interlayer sites sandwiched between the tetrahedral sheets (Fig. 4; Table 2). The two Na sites are both dominated by Na atoms in a distorted octahedral coordination, with <Na – O> distances of 2.453 and 2.535 Å, respectively (Table 3). A site-occupancy refinement revealed that all Ca (0.56 apfu) is ordered in the Na2 site (Table 4). There are also two Sr sites that are both dominated by Sr atoms and coordinated by eight O atoms in a square-antiprismatic arrangement with <Sr – O> distances of 2.634 and 2.624 Å, respectively (Table 3). There is a slight deficit in scattering at the Sr2 site relative to 100% Sr occupancy, which most likely stems from the presence of K and vacancies in this site (Table 4). There are four unique Si tetrahedra with <Si – O> distances ranging from

1.625 to 1.634 Å; both site scattering and <Si – O> distances suggest that the Si sites are occupied primarily by Si. A single larger tetrahedron (<Fe – O> = 1.941 Å) has a refined site scattering of 47.59(8) electrons per formula unit (epfu), in reasonable agreement with the assignment of all Fe + Mn + Zn + Mg + Ti, and some of the Al from the chemical analysis to this site (Table 4). The <Fe – O> distance calculated assuming the Fe^{2+}/Fe^{3+} ratio obtained from the Mössbauer analysis is 1.952 Å (i.e., 0.572 + 1.38 Å), which is also in agreement with the observed <Fe – O> distance of 1.941 Å. The Fe tetrahedron is thus occupied by ~60% divalent cations (predominantly Fe^{2+}) and 40% trivalent cations (mostly Fe^{3+}), providing further support for the proposed end-member formula (see above).

X-RAY POWDER DIFFRACTION

An X-ray diffraction (XRD) pattern was measured with a Bruker D8 Discover SuperSpeed micro-powder diffractometer equipped with a Cu$K\alpha$ source, multi-wire 2D detector and modified Gandolfi attachment. In addition, a pseudo-powder XRD pattern was collected in situ from a polished section using a Rigaku D-max Rapid micro-diffractometer equipped with a curved-image-plate detector, variety of beam collimators and motorized stage allowing two angular movements. The data were collected in reflection mode using various sample-to-beam geometries and operating conditions. The patterns obtained by the two techniques are very similar, but the in situ measurements did not detect, or underestimated the intensity of, low-angle reflections (d > 4 Å), and showed strong preferred-orientation effects owing to the subparallel alignment of vladykinite crystals in the sample. The measured XRD micro-powder pattern and interplanar spacings calculated on the basis of structural data are given in Table 5. The unit-cell parameters, refined from the powder XRD data by least-squares techniques, are in good agreement with those determined by single-crystal techniques: a = 5.215(2), b = 7.897(6), c = 26.05(2) Å, β = 90.21(5)°, V = 1072.6(7) $Å^3$.

DISCUSSION

Relation to other mineral species

Only a small number of phyllosilicate minerals contain complex tetrahedral sheets comprising four-, five- and eight-membered rings, as in vladykinite (Fig. 4). The simplest arrangement, consisting of zigzag silicate chains $(Si_6O_{17})^{10-}$ running parallel to [001] and connected into a sheet by larger $(Zn,Fe,Mn,Mg)O_4$ tetrahedra, was reported in the crystal structure of nordite-(Ce) and related minerals (Bakakin et al. 1970; Pushcharovsky et al. 1999). Their general formula can be written as $Na_3SrLREE(Zn,Fe^{2+},Mn,Mg)Si_6O_{17}$, where LREE is a light rare-earth element. A topologically similar sheet (ring symbol $4^15^28^1$) was recently identified in the structure of bussyite-(Ce) $REE_2CaNa_6MnBe_5Si_9(O,OH)_{30}(F,OH)_4$, where all tetrahedra are similar in size and populated by Si, Be or both (Grice et al. 2009). The pattern of Be distribution within the sheet in bussyite-(Ce) is also different from the distribution of tetrahedrally coordinated divalent cations in the nordites (Figs. 5a and 5b), but the stoichiometry of the sheet is preserved. A completely different arrangement of silicate rings and stoichiometry are found in the beryllosilicates semenovite-(Ce), $Na_{0-2}(Ca,Na)_8REE_2(Fe^{2+},Mn,Zn)(Be,Si)_{20}(O,OH,F)_{48}$ (Mazzi et al. 1979) and harstigite, $Ca_6MnBe_4Si_6O_{22}(OH)_2$ (Hesse and Stümpel 1986). In contrast to the nordites, Mn and other divalent cations larger than Be, but smaller than Ca occupy octahedral sites in bussyite-(Ce), semenovite-(Ce) and harstigite. Although tetrahedral sheets in the structure of vladykinite show the same 1:4:1 proportion among four-, five- and eight-membered rings and, hence, the same stoichiometry as in semenovite-(Ce) or harstigite (i.e. 10 tetrahedrally coordinated cations per 24 anions), they are topologically unique (cf. Figs. 5c and 5d). The structure of vladykinite does not appear to have any known natural or synthetic analogues at present, but shows a clear structural affinity to the nordites. The $4^15^48^1$ sheet in vladykinite can be visualized as consisting of eight-tetrahedra-long segments of nordite-like chains, $(Si_8O_{24})^{16-}$ interconnected by sharing all of their available vertices with FeO_4 tetrahedra (Figs. 4, 5a and 5d). In both structure types, tetrahedral sheets are sandwiched between layers of NaO_6 octahedra and SrO_8 ($\pm$ $LREEO_8$) square

antiprisms. The $Na1O_6$, $Na2O_6$ and SrO_8 polyhedra are very similar in vladykinite and ferronordite-(Ce), whereas the FeO_4 tetrahedron is somewhat larger in the latter mineral because it accommodates only Fe^{2+} and other divalent cations (Pushcharovsky et al. 1999; Table 3).

Paragenesis

In the host lujavrite, vladykinite is a relatively early liquidus phase precipitated after lamprophyllite, but prior to potassium feldspar, Sr-bearing eudialyte and aegirine. The high modal content of lamprophyllite, eudialyte and vladykinite, along with the presence of K-rich vishnevite and strontianite, in this rock are undoubtedly due to the extremely evolved, volatile-rich nature of its parental peralkaline melt. The lack of Ba silicates in the lujavrite, and low Ba contents in its constituent minerals (0.9-1.8 wt.% BaO in lamprophyllite, 0.2 wt.% in vladykinite, and below detection in the feldspar) suggest that this melt was derived from a more primitive magma by fractional crystallization of potassium feldspar, in which Ba is much more compatible than Sr (Henderson and Pierozynski 2012); BaO values up to 3 wt.% were reported in syenitic feldspars from Murun by Konev et al. (1996) and Reguir (2001). The evolution of the lujavrite culminated with the release of a sulfate-carbonate-rich fluid, which reacted with the early magmatic mineral assemblage to produce vishnevite and strontianite. At this stage, vladykinite became chemically unstable and underwent pseudomorphization by strontianite (Fig. 1). Precipitation of $SrCO_3$ and removal of silica during the replacement imply alkaline conditions, but a quantitative assessment of these conditions cannot be made at present because thermodynamic data for vladykinite are not available. Similar late-stage processes have been documented elsewhere at Maly Murun, where strontianite developed at the expense of fluorapatite and fluorstrophite (Chakhmouradian et al. 2002).

ACKNOWLEDGEMENTS

This work was supported by the Natural Sciences and Engineering Research Council of Canada and Canada Foundation for Innovation. The authors are grateful to Frank C. Hawthorne, for access to the X-ray facilities at the University of Manitoba. Panseok Yang is thanked for his

help with LA-ICP-MS. We also acknowledge Sergey Krivovichev and two anonymous referees for their constructive comments on the earlier version of this manuscript, and Associate Editor Hongwu Xu for speedy handling.

REFERENCES CITED

Ageeva, O.A. and Borutzky, B.Ye. (2004) Kalsilite in the rocks of Khibiny massif: morphology, paragenesis, genetic conditions. New Data on Minerals, 39, 40-49.

Bakakin, V.V., Belov, N.V., Borisov, S.V., and Solovyeva, L.P. (1970) The crystal structure of nordite and is relationship to melilite and datolite-gadolinite. American Mineralogist, 55, 1167-1181.

Chakhmouradian, A.R., Reguir, E.P., and Mitchell, R.H. (2002) Strontium-apatite: New occurrences, and the extent of Sr-for-Ca substitution in apatite-group minerals. Canadian Mineralogist, 40, 121-136.

Deer, W.A., Howie, R.A., and Zussman, J. (1997) Rock-forming Minerals. Volume 1A: Orthosilicates. The Geological Society, Bath, UK, 932 pp.

Evdokimov, M.D. (1995) Charoite: a unique mineral from a unique occurrence. World of Stones, 1995 (7), 3-11.

Grice, J.D., Rowe, R., Poirier, G., Pratt, A., and Francis, J. (2009) Bussyite-(Ce), a new beryllium silicate mineral species from Mont Saint-Hilaire, Quebec. Canadian Mineralogist, 47, 193-204.

Henderson, C.M.B. and Pierozynski, W.J. (2012) An experimental study of Sr, Ba and Rb partitioning between alkali feldspar and silicate liquid in the system nepheline – kalsilite – quartz at 0.1 GPa $P(H_2O)$: a revisitation and reassessment. Mineralogical Magazine, 76, 157-190.

Hesse, K.-F. and Stümpel, G. (1986) Crystal structure of harstigite, $MnCa_6Be_4[SiO_4]_2[Si_2O_7]_2(OH)_2$. Zeitschrift für Kristallographie, 177, 143-148.

Konev, A.A., Vorob'ev, E.I., and Lazebnik, K.A. (1996) Mineralogy of the Murun Alkaline Massif. Siberian Branch RAS press, Novosibirsk, Russia, 221 pp. (in Russian).

Kostyuk, V.P., Panina, L.I., Zhidkov, A.Ya., Orlova, M.P., and Bazarova, T.Yu. (1990) Potassic Alkaline Magmatism of the Baikal-Stanovoy Rift System. Nauka, Novosibirsk, Russia, 237 pp. (in Russian).

Mazzi, F., Ungaretti, L., and Dal Negro, A. (1979) The crystal structure of semenovite. American Mineralogist, 64, 202-210.

Mitchell R.H. and Vladykin N.V. (1993) Rare-earth element-bearing tausonite and potassium barium titanates from the Little Murun potassic alkaline complex. Mineralogical Magazine, 57, 651-668.

___ (1996) Compositional variation of pyroxene and mica from the Little Murun ultrapotassic complex, Aldan Shield, Russia. Mineralogical Magazine, 60, 907-925.

Pakhomovsky, Ya.A., Yakovenchuk, V.N., and Ivanyuk, G.Yu. (2009) Kalsilite of the Khibiny and Lovozero alkaline plutons, Kola Peninsula. Geology of Ore Deposits, 51, 822-826.

Pekov, I.V., Olysych, L.V., and Chukanov, N.V. (2011) Crystal chemistry of cancrinite-grpup minerals with an *AB*-type framework: a review and new data. I. Chemical and structural variations. Canadian Mineralogist, 49, 1129-1150.

Pushcharovsky, D.Yu., Pekov, I.V., Pluth, J.J., Smith J.V., Ferraris, G., Vinogradova, S.A., Arakcheeva, A.V., Soboleva, S.V., and Semenov, E.I. (1999) Raite, manganonordite-(Ce) and ferronordite-(Ce) from the Lovozero massif: crystal structures and mineralogical geochemistry. Crystallography Reports, 44, 565-574.

Reguir, E.P. (2001) Aspects of the Mineralogy of the Murun Alkaline Complex, Yakutia, Russia. Unpublished MSc Thesis, Lakehead University, Thunder Bay, Canada, 193 pp.

van Achterbergh, E., Ryan, C.G., and Griffin, W.L. (2001) GLITTER on-line interactive data reduction for the LA-ICPMS microprobe. Macquarie Research Ltd., Sydney.

Vladykin N.V. (1981) Geology of the Murun massif, the place of pseudoleucite (synnyrite-like) syenites in the massif, and their chemical composition. In Problemy Osvoeniya Zony BAM. Novosibirsk, Russia, 106-113 (in Russ.).

____ (1997) Geochemistry and genesis of lamproites of the Aldan Shield. Russian Geology and Geophysics, 38, 128-141.

____ (2009) Potassium alkaline lamproite-carbonatite complexes: petrology, genesis, and ore reserves. Russian Geology and Geophysics, 50, 1119-1128.

Vladykin N.V. and Tsaruk I.I. (2003) Geology, chemistry and genesis of Ba-Sr-bearing ("benstonite") carbonatites of the Murun Massif. Russian Geology and Geophysics, 44, 315-330.

FIGURE CAPTIONS

Figure 1. (a) Prismatic crystals of vladykinite (Vld) showing turbid areas of partial replacement by strontianite (Str); the matrix is predominantly potassium feldspar (Kfs); cross-polarized light. (b) Pseudomorphs of strontianite (Str) after vladykinite associated with eudialyte (Eud) and lamprophyllite (Lmp); back-scattered-electron image. Scale bar is 0.2 mm for both images.

Figure 2. Raman spectrum of vladykinite (analysis spot indicated by a star in the inset).

Figure 3. ^{57}Fe Mössbauer spectrum of vladykinite.

Figure 4. The crystal structure of vladykinite viewed perpendicular to (100), showing complex sheets of SiO_4 and (Fe,Mn,Zn,Al)O_4 tetrahedra (*Fe*O_4) and locations of *Na* and *Sr* sites. The unit cell is outlined.

Figure 5. Comparison of the tetrahedral sheet topology in the structures of: (a) ferronordite-(Ce) and related minerals (Pushcharovsky et al. 1999); (b) bussyite-(Ce) (Grice et al. 2009); (c) semenovite-(Ce) (Mazzi et al. 1979); and (d) vladykinite (this work). Silicon atoms are indicated by empty circles, and other tetrahedrally coordinated cations [i.e. mostly Be in bussyite-(Ce) and semenovite-(Ce); Fe^{2+}, Mn and Zn in the nordites; Fe^{2+} and Fe^{3+} in vladykinite] by filled circles.

APPENDIX 1 (ONLINE)

Mineralogy of alkaline igneous and associated hydrothermal and metasomatic rocks, Murun complex, eastern Siberia, Russia.

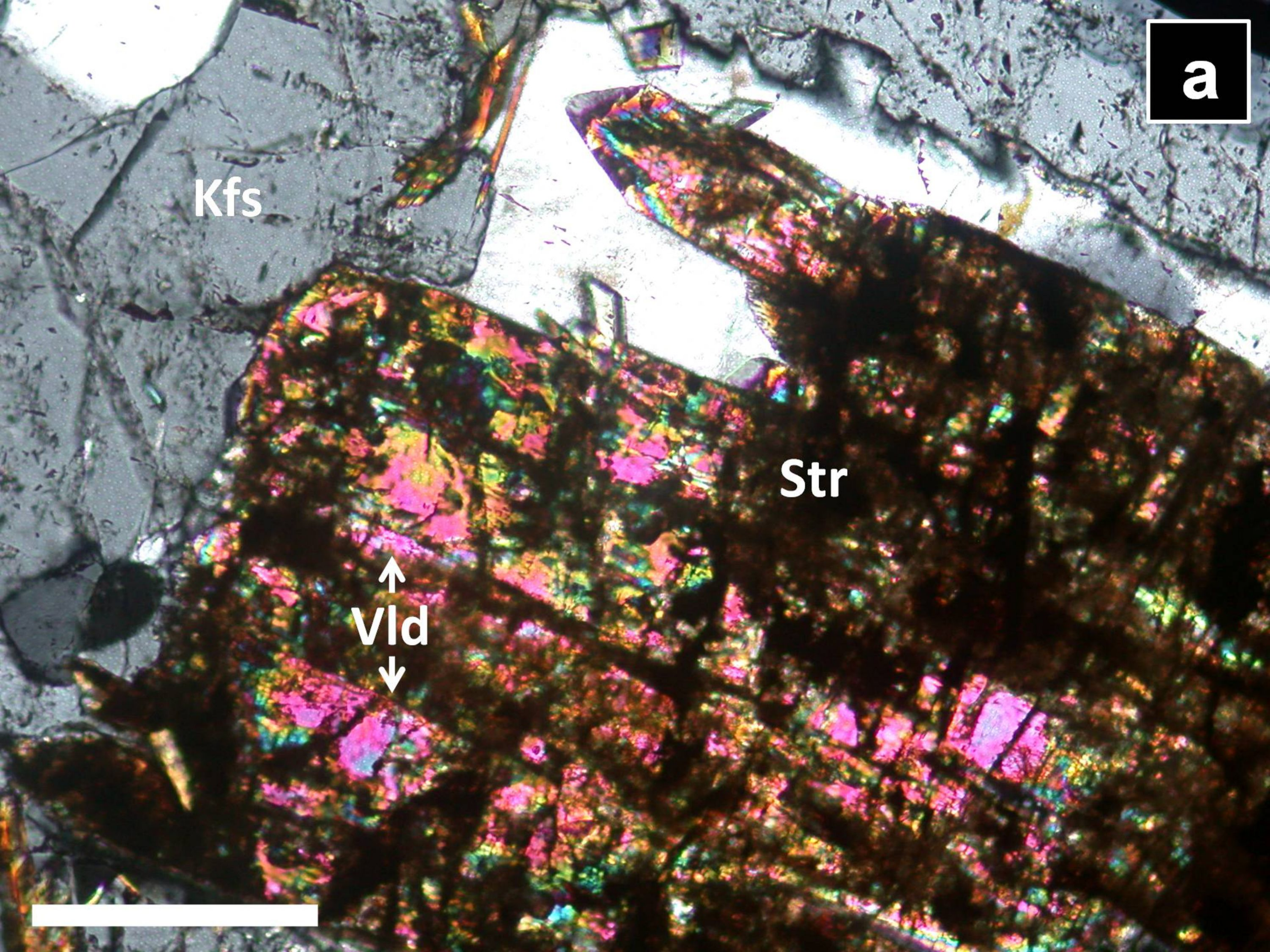
a
Kfs
Str
Vld

b

Kfs

Eud

Lmp

Str

LabRam Aramis (Jobin-Yvon Horiba), 532 nm laser, cooled CCD detector
Measured in confocal mode with a 1800 gr/mm grating, 100 μm hole, and ×100 objective
Calibrated to crystalline Si standard (520.7 cm^{-1} signal)

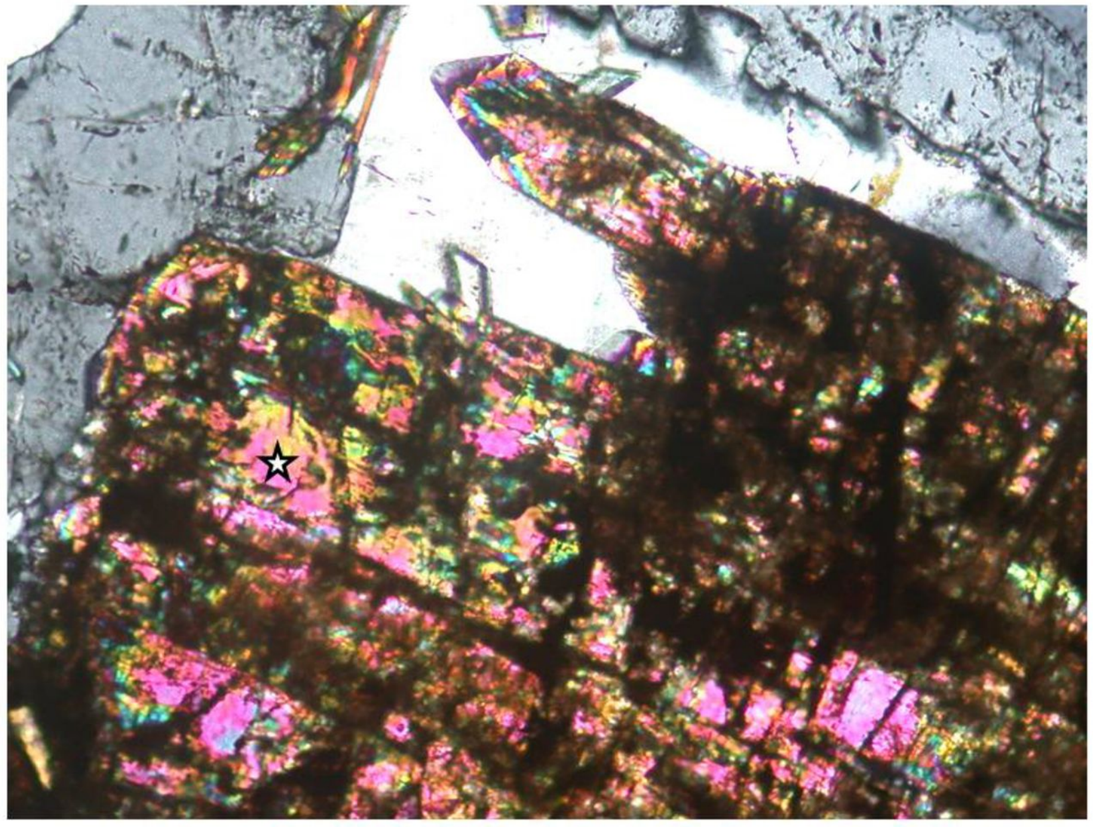

Intensity (arb. units)

203
401
465
991
348
968
167
264
129
915
681
1039

O-H stretching range

200
800
1400
2000
2600
3200
3800

Raman shift, cm^{-1}

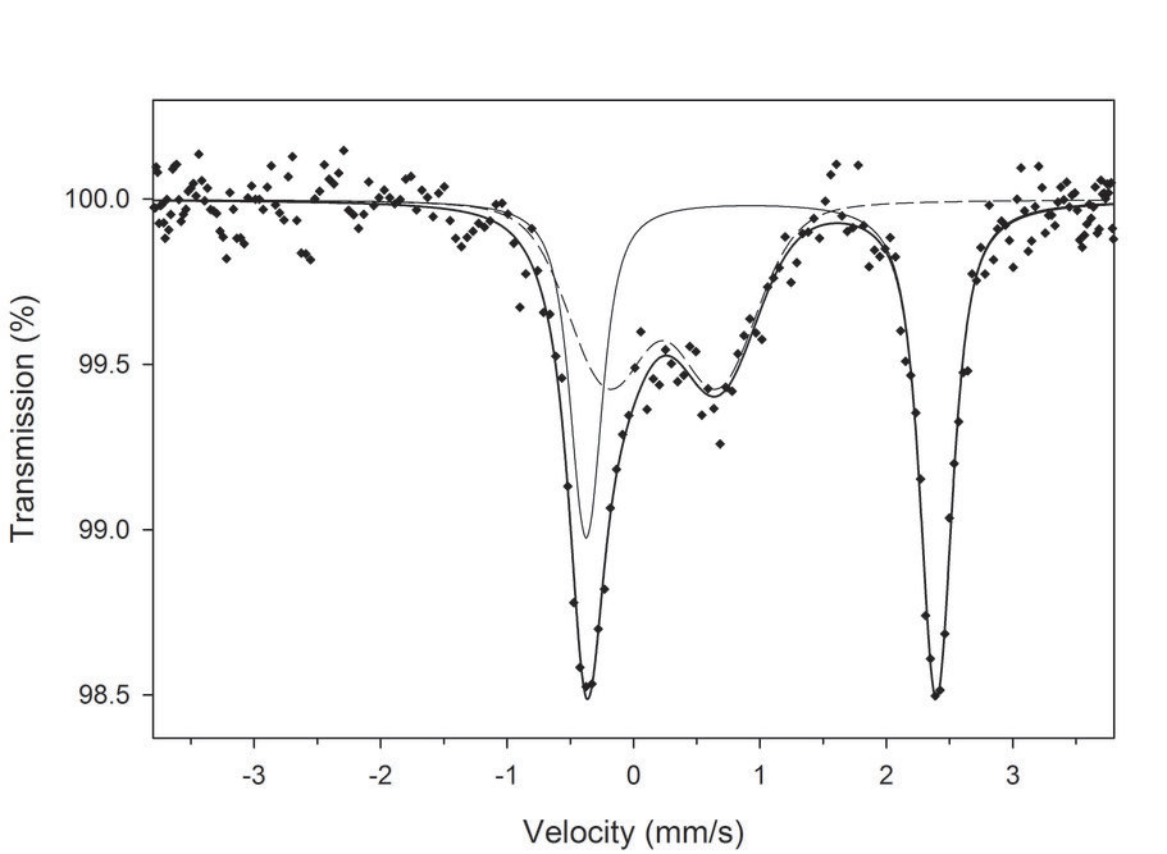
Transmission (%)
100.0
99.5
99.0
98.5
-3
-2
-1
0
1
2
3
Velocity (mm/s)

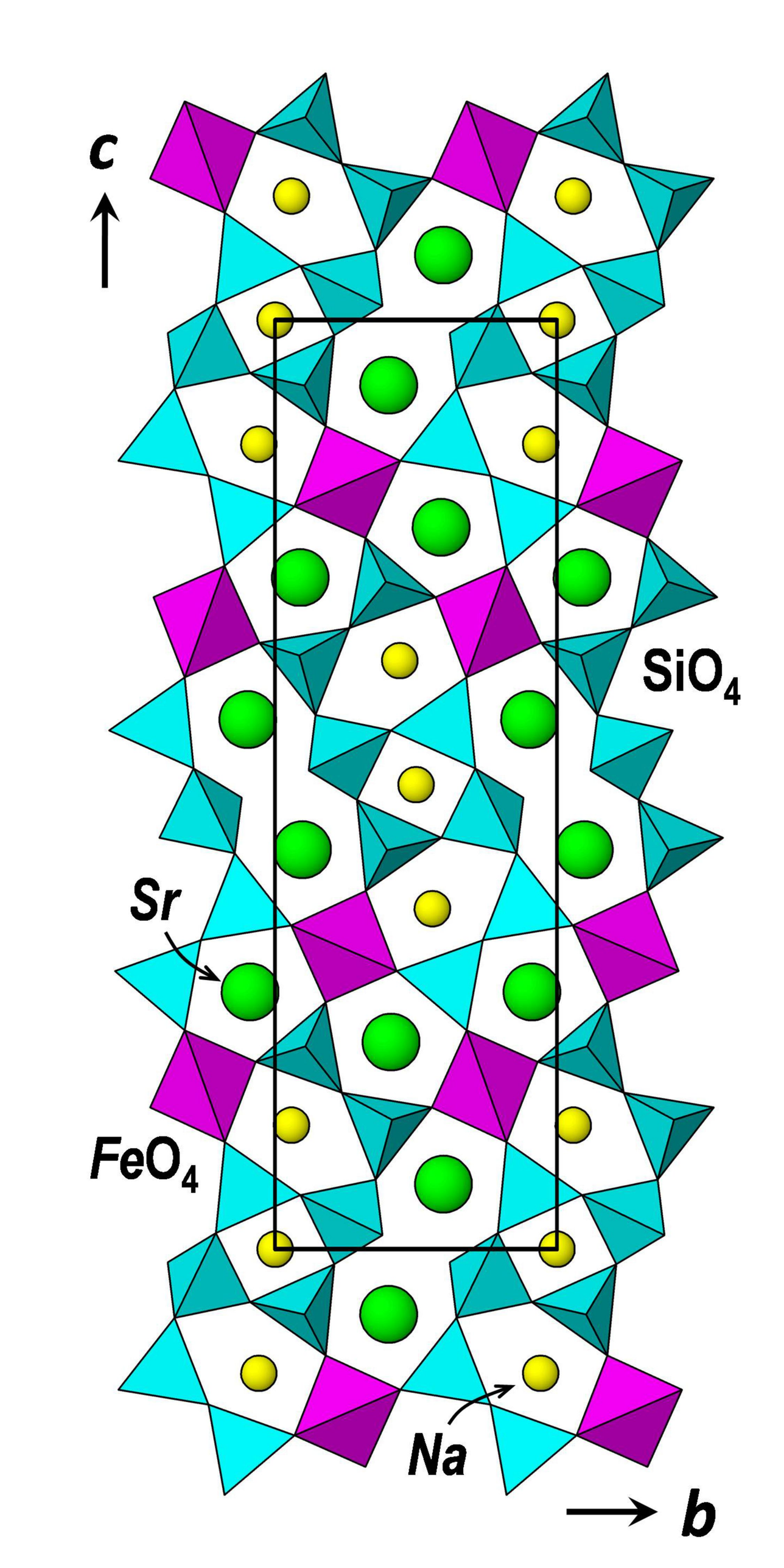
c
SiO4
Sr
FeO4
Na
b

a

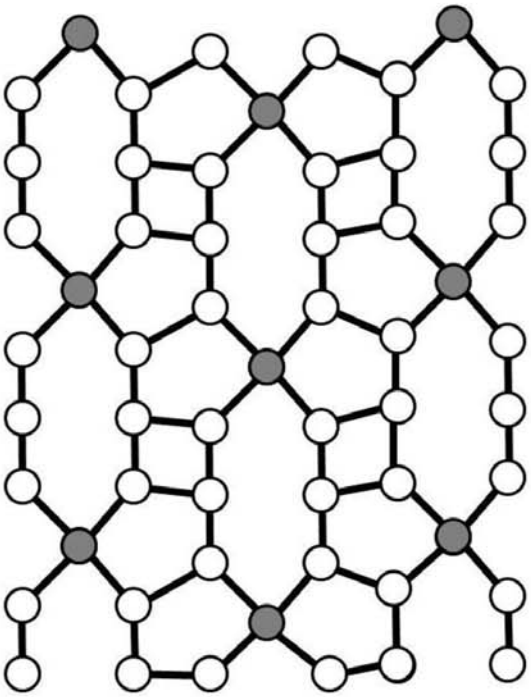

Nordites: $4^{1}5^{2}8^{1}$

b

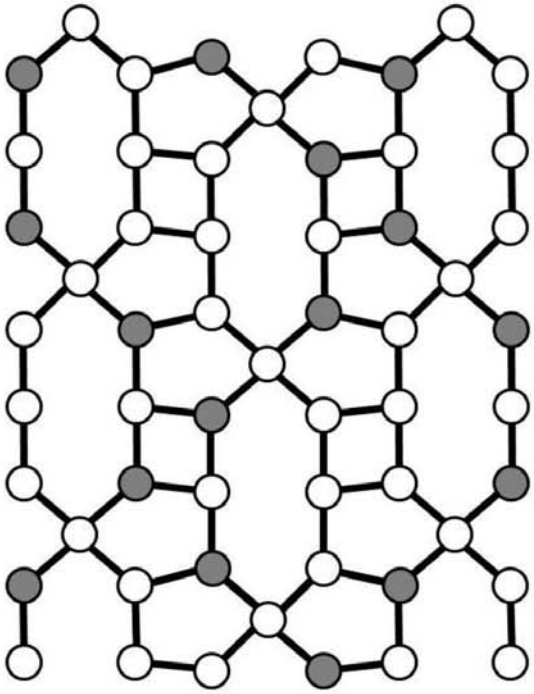

Bussyite-(Ce): $4^{1}5^{2}8^{1}$

c

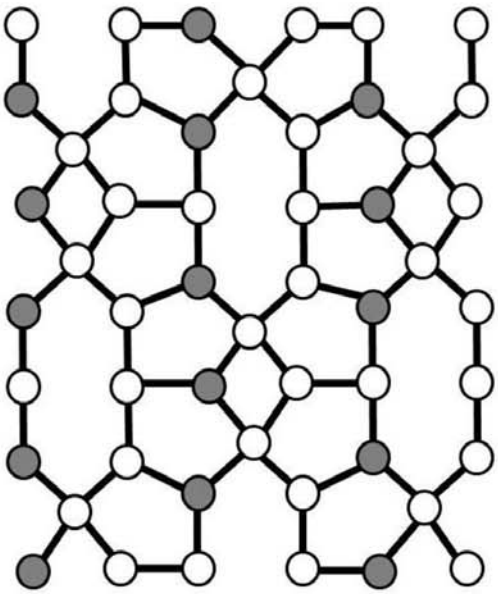

Semenovite-(Ce): $4^{1}5^{4}8^{1}$

d

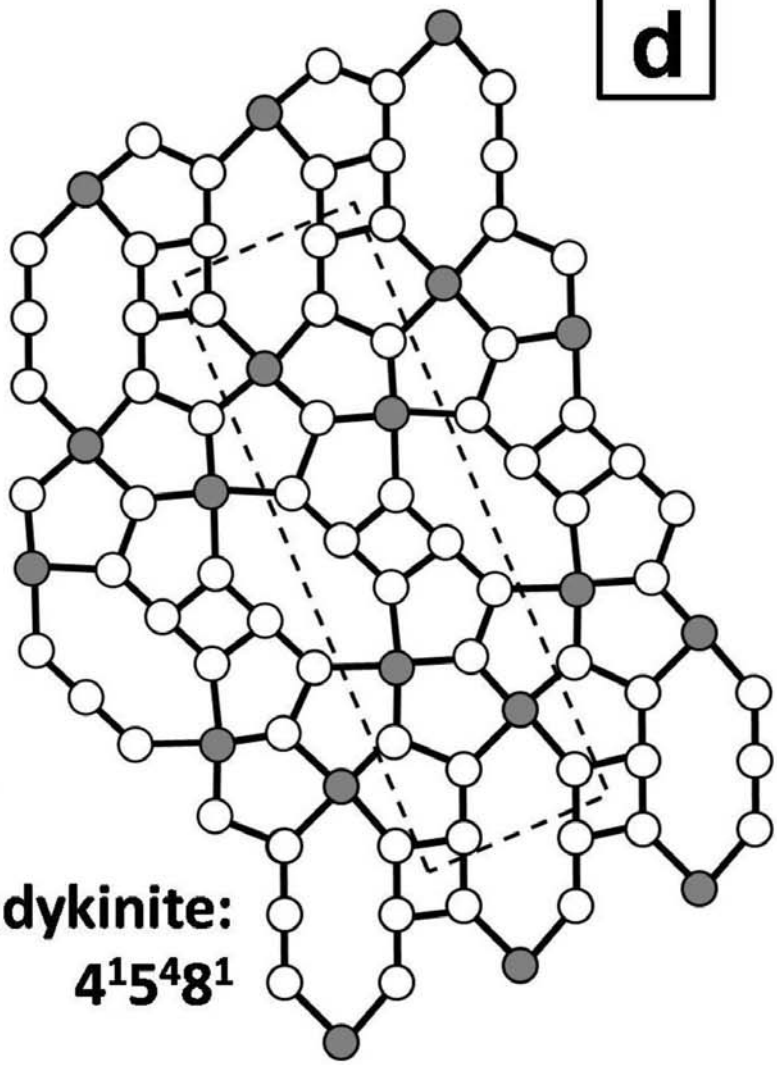

Vladykinite: $4^{1}5^{4}8^{1}$

Table 1. Mean chemical composition of vladykinite

Oxide*	**wt.%**	**range**	**ESD**
Na_2O	6.74	6.41-7.18	0.21
MgO	0.14	0.13-0.15	0.01
Al_2O_3	1.38	1.21-1.70	0.15
SiO_2	41.66	41.03-42.32	0.39
K_2O	0.16	0.15-0.17	0.01
CaO	2.77	2.58-2.96	0.09
TiO_2	0.10	0.07-0.14	0.02
MnO	1.60	1.41-1.72	0.10
FeO_T[#]	8.98	8.64-9.29	0.19
ZnO	1.33	1.06-1.75	0.25
SrO	34.99	34.28-35.92	0.47
La_2O_3	0.22	0.11-0.33	0.08
Ce_2O_3	0.16	0-0.34	0.09
Total	**98.90**		
Element‡	**ppm**	**range**	**ESD**
Mg	1010	903-1220	122
Sc	0.52		0.08
Mn	12683	11217-14005	1143
Co	29	28-32	2
Zn	9515	7899-11818	1581
Y	1.02	0.93-1.11	0.07
Ba	1838	1402-2194	312
La	2776	1949-3553	761
Ce	1709	1138-2361	575
Pr	74	44-108	28
Nd	101	58-148	41
Sm	2.4	1.4-3.9	0.9
Eu	0.37	0.17-0.60	0.14
Gd	48	32-65	14
Pb	12.9	11.8-14.2	0.9
Th	22	6-37	12
U	0.27	0.04-0.90	0.32

***** Based on 16 WDS analyses.

[#] Based on the Mössbauer data, FeO_T should be recast into FeO (4.76 wt.%) and Fe_2O_3 (4.69 wt.%).

‡ Based on six LA-ICP-MS analyses.

Table 2. The crystal structure of vladykinite: atomic coordinates and displacement parameters

Site	*x*	*y*	*z*	U_{eq}, Å^2
Na1	½	½	½	0.0278(3)
Na2	0.48483(11)	0.44221(9)	0.63351(2)	0.0210(2)
Sr1	0.49578(3)	0.90294(2)	0.57005(1)	0.01107(5)
Sr2	0.50609(3)	0.58890(2)	0.77700(1)	0.01184(6)
Fe	0.00453(5)	0.75589(3)	0.67545(1)	0.01134(9)
Si1	0.94527(9)	0.39083(6)	0.71424(2)	0.01073(9)
Si2	0.95867(8)	0.10612(6)	0.63401(2)	0.01018(9)
Si3	0.05166(8)	0.23197(6)	0.53139(2)	0.00944(9)
Si4	0.02973(8)	0.60042(5)	0.56752(2)	0.00895(8)
O1	0.2495(2)	0.39304(17)	0.71818(5)	0.0175(3)
O2	0.8052(2)	0.56879(16)	0.70091(5)	0.0180(2)
O3	0.7963(2)	0.32075(17)	0.76480(5)	0.0170(2)
O4	0.8411(2)	0.26336(17)	0.66773(5)	0.0169(2)
O5	0.7412(2)	0.58495(19)	0.86101(5)	0.0209(2)
O6	0.7921(2)	- 0.05618(16)	0.65173(5)	0.0161(2)
O7	0.8648(2)	0.14346(16)	0.57432(4)	0.0138(2)
O8	0.2852(2)	0.11891(16)	0.51492(5)	0.0155(2)
O9	0.1552(2)	0.41060(14)	0.55787(5)	0.0131(2)
O10	0.1358(2)	0.71048(16)	0.51702(4)	0.0131(2)
O11	0.7275(2)	0.60334(15)	0.57060(5)	0.0140(2)
O12	0.1881(2)	0.67881(16)	0.61515(5)	0.0145(2)

Table 3. Selected bond distances (Å) in the crystal structure of vladykinite; mean distances for ferronordite-(Ce) are provided for comparison

2 × Na1 – O9	2.4589(12)	Na2 – O1	2.5634(14)
2 × Na1 – O10	2.5666(12)	Na2 – O2	2.6172(15)
2 × Na1 – O11	2.3326(12)	Na2 – O4	2.4962(14)
		Na2 – O9	2.6208(13)
		Na2 – O11	2.4384(14)
		Na2 – O12	2.4738(14)
<Na1 – O>	2.453	<Na2 – O>	2.535
Sr1 – O5	2.6200(13)	Sr2 – O1	2.5540(13)
Sr1 – O6	2.6443(13)	Sr2 – O1	2.7262(13)
Sr1 – O7	2.7082(12)	Sr2 – O2	2.5371(13)
Sr1 – O8	2.4852(12)	Sr2 – O3	2.6271(13)
Sr1 – O8	2.5060(12)	Sr2 – O3	2.6497(13)
Sr1 – O10	2.7792(12)	Sr2 – O4	2.7010(13)
Sr1 – O11	2.6611(12)	Sr2 – O5	2.5049(13)
Sr1 – O12	2.6697(13)	Sr2 – O6	2.6887(13)
<Sr1 – O>	2.634	<Sr2 – O>	2.624
Si1 – O1	1.5887(13)	Si2 – O4	1.6447(13)
Si1 – O2	1.6231(14)	Si2 – O5	1.5781(13)
Si1 – O3	1.6320(13)	Si2 – O6	1.6194(14)
Si1 – O4	1.6662(13)	Si2 – O7	1.6563(12)
<Si1 – O>	1.628	<Si2 – O>	1.625
Si3 – O7	1.6455(12)	Si4 – O9	1.6583(12)
Si3 – O8	1.5729(13)	Si4 – O10	1.6763(12)
Si3 – O9	1.6620(13)	Si4 – O11	1.5786(13)
Si3 – O10	1.6562(12)	Si4 – O12	1.6118(12)
<Si3 – O>	1.634	<Si4 – O>	1.631
Fe – O2	1.9293(14)		
Fe – O3	1.9368(13)		
Fe – O6	1.9527(13)		
Fe – O12	1.9447(12)		
<Fe – O>	1.941		

Ferronordite-(Ce), Pushcharovsky et al. (1999):

<Na1 – O>	2.419	<Na2 – O>	2.527
<Sr – O>	2.629	<REE – O>	2.546
<Si1 – O>	1.634	<Si1 – O>	1.629
<Si3 – O>	1.639	<Fe – O>	1.981

Table 4. Calculated cation-site occupancies in the crystal structure of vladykinite

Site	Occupancy (from WDS and LA-ICP-MS)	Scattering, epfu calculated	Scattering, epfu observed, SCSR*
Na1	Na	11	11
Na2	$Na_{1.45}Ca_{0.56}$	27.2	27.90(9)
Sr1	Sr_2	76	76
Sr2	$Sr_{1.84}K_{0.04}La_{0.02}Ce_{0.01}[\ ]_{0.10}$	72.4	70.46(8)
Fe	$Fe^{2+}_{0.75}Fe^{3+}_{0.66}Mn_{0.26}Zn_{0.16}Al_{0.12}Mg_{0.05}Ti_{0.01}$	50.3	47.59(8)

* SCSR = single-crystal structure refinement.

Table 5. Powder XRD pattern of vladykinite

I_{meas}	d_{meas}, Å	d_{calc}, Å	h	k	l
19	7.523	7.557	0	1	1
9	6.692*	6.752	0	1	2
6	5.839	5.842	0	1	3
5	5.167*	5.215	1	0	0
14	5.011	5.024	0	1	4
30	**4.290**	**4.295**	**-1**	**1**	**1**
		4.290	**1**	**1**	**1**
8	4.059	4.063	1	0	4
9	3.894	3.904	0	2	1
		3.895	-1	1	3
58	**3.612**	**3.623**	**-1**	**1**	**4**
		3.613	**1**	**1**	**4**
30	**3.339**	**3.342**	**-1**	**0**	**6**
		3.335	**1**	**1**	**5**
		3.330	**1**	**0**	**6**
7	3.258	3.256	0	0	8
37	**3.146**	**3.148**	**1**	**2**	**0**
100	**2.957**	**2.962**	**-1**	**2**	**3**
		2.957	**1**	**2**	**3**
100	**2.826**	**2.832**	**-1**	**1**	**7**
		2.824	**1**	**1**	**7**
28	**2.604**	**2.608**	**2**	**0**	**0**
5	2.553	2.551	-1	2	6
32	**2.470**	**2.476**	**2**	**1**	**0**
		2.473	**0**	**1**	**10**
25	**2.437**	**2.440**	**0**	**3**	**4**
14_B	2.391*	2.406	-1	2	7
		2.401	1	2	7
		2.383	-2	1	3
10_B	2.334*	2.350	1	3	0
		2.334	-1	0	10
		2.327	1	0	10
		2.313	-1	3	2
16	2.109	2.112	-2	2	3
		2.109	2	2	3
18	2.063	2.065	-2	1	7
		2.058	2	1	7
10_B	1.944*	1.948	-2	2	6
		1.942	0	1	13
		1.925	0	4	3
8	1.893	1.894	-1	2	11
		1.890	1	2	11
17	1.852	1.851	0	3	10
24	1.800	1.798	-2	1	10
		1.797	0	4	6

I_{meas}	d_{meas}, Å	d_{calc}, Å	h	k	l
25	**1.785**	**1.791**	**2**	**1**	**10**
		1.783	**-2**	**3**	**4**
		1.781	**2**	**3**	**4**
15	1.743	1.746	-1	3	10
		1.743	1	3	10
11	1.684	1.683	0	2	14
4	1.639	1.641	3	1	4
5	1.616	1.616	-3	0	6
4	1.593	1.591	-3	2	0
8	1.565	1.566	-3	2	3
		1.564	3	2	3
5	1.548	1.547	-3	1	7

Notes: B = broad reflection;
* = reflection not used in the cell refinement